Supporting Information

Impact of Liquid Phase Formation on Microstructure and Conductivity of Li-Stabilized Na-β”-alumina Ceramics

Marie-Claude Bay[1,2], Meike V. F. Heinz[1], Renato Figi[1], Claudia Schreiner[1], Diego Basso[3], Nicola Zanon[3], Ulrich F. Vogt[1,2] ,Corsin Battaglia[1]*

[1] Empa, Swiss Federal Laboratories for Materials Science and Technology, Überlandstrasse 129, 8600 Dübendorf, Switzerland

[2] Institute for Environment and Natural Resources, Albert-Ludwigs-University Freiburg, Crystallography, 79098 Freiburg im Breisgau, Germany

[3] FZSONICK SA, 6855 Stabio, Switzerland

* Meike.Heinz@empa.ch

A. Measurement of ion conductivity

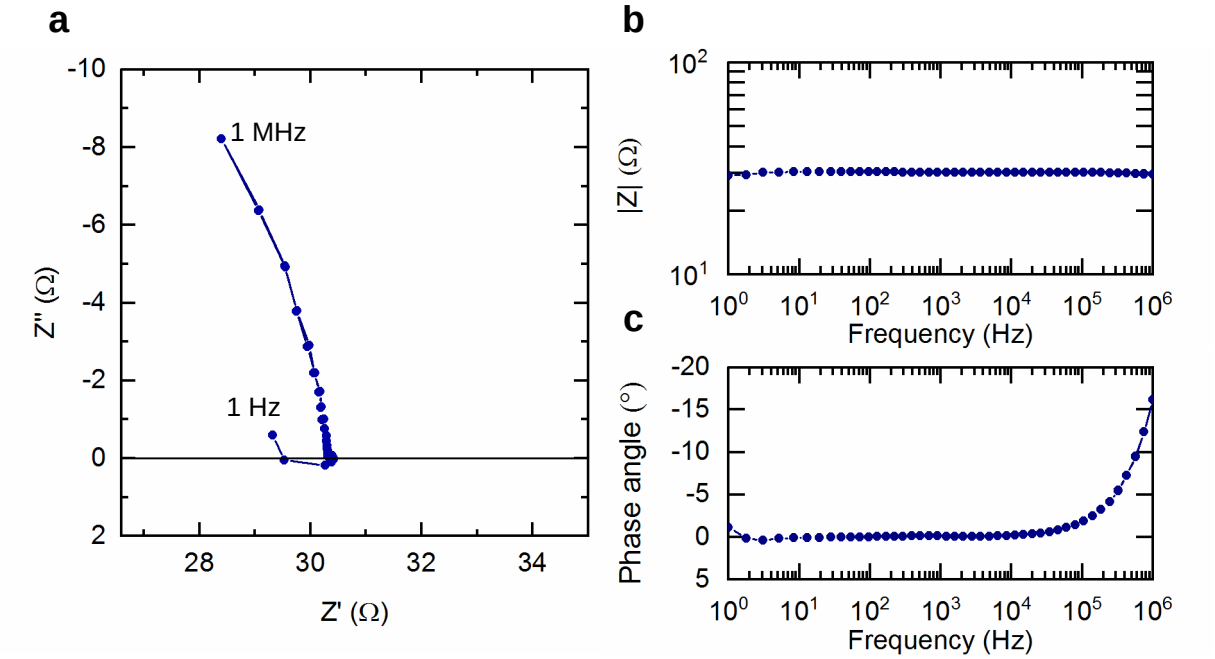

Figure S1 *Typical impedance response for Na-β''-alumina ceramics at 300 °C. (a) Real (Z') vs imaginary (Z'') part of impedance. (b) Impedance modulus and (c) phase angle vs frequency. The response in the Hz-kHz range is typical of a resistor and is ascribed to the ion conduction in the electrolyte.*

B. Investigation of the liquid phase formation

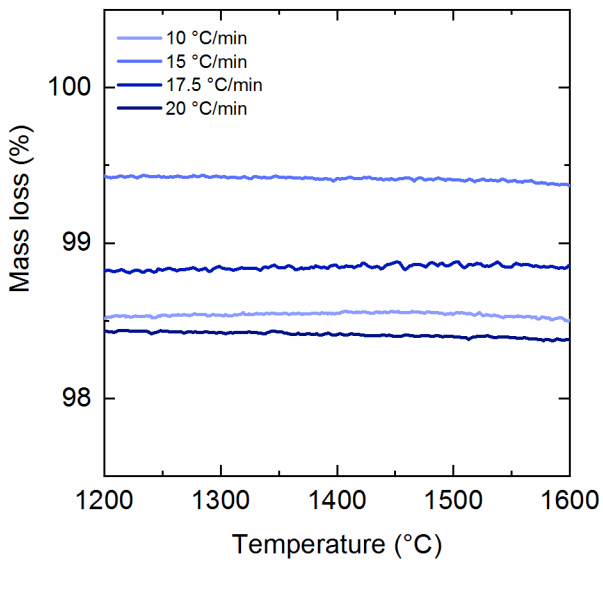

Figure S2 *Thermogravimetric analysis of the starting powder for different heating rates. No mass loss is observed at the temperature of the liquid phase formation of 1503 °C.*

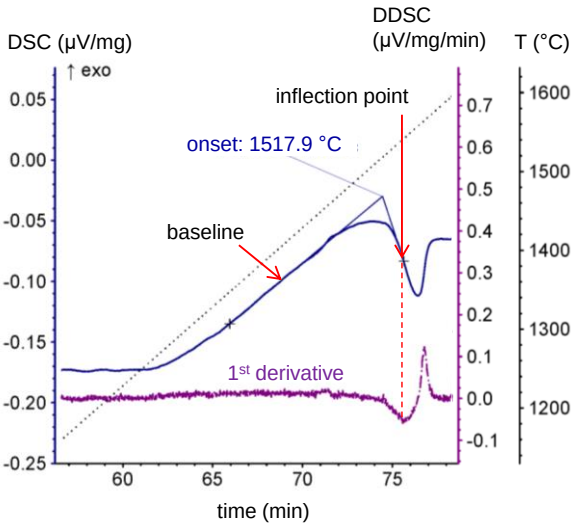

Figure S3 *Differential scanning calorimetry measured at a rate of 20 °C/min. The onset temperature of the liquid phase formation is determined at the intersection of the baseline with the tangent at the inflection point of the peak.*

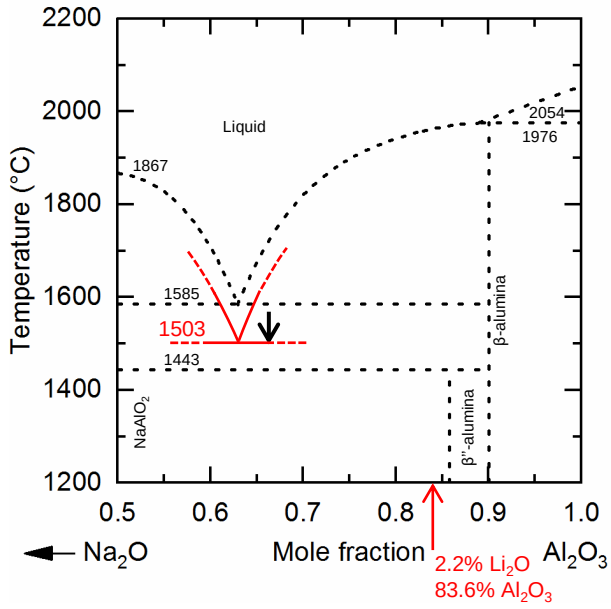

Figure S4 *Binary phase diagram Na_2O – Al_2O_3 (dashed black lines, adapted from [34]) and implications for a ternary composition with 2.2 mol % Li-doped Na-β''-alumina (red plane lines), for which a eutectic temperature of 1503 °C is determined. Note that the exact composition of this point in the ternary phase diagram may deviate from the binary eutectic composition.*

C. β/ β''-alumina content

β''-alumina fractions reported in literature are not based on Rietveld refinements analyzing the whole diffraction pattern, but rather on the comparison of selected peak intensities. This may lead to variable results, as different approaches were proposed in literature to determine the β-alumina fraction. The approach was originally presented by Pekarsky [35], but has since been applied in different variations, some including β- and β''-alumina references patterns, some not [20][36]:

$$f(\beta'') = 1 - \frac{I(\beta_{sample})}{I(\beta_{sample}) + \frac{I(\beta_{ref})}{I(\beta''_{ref})} I(\beta''_{sample})} \quad (3)$$

$$f(\beta'') = 1 - \frac{I(\beta_{sample})}{I(\beta_{sample}) + I(\beta''_{sample})} \quad (4)$$

$$f(\beta'') = 1 - \frac{I(\beta_{sample})}{I(\beta''_{sample})} \quad (5)$$

where $I(\beta_{sample})$ and $I(\beta''_{sample})$ are the peak intensities of the β- and β''-alumina phases in the sample, and $I(\beta_{ref})$, $I(\beta''_{ref})$ are the peak intensities of β- and β''-alumina phases in reference diffraction patterns. The most frequently applied approach to report the β''-content in recent literature is according to equation 3 [37][38][39].

To assess the variability of results obtained by the different approaches, we apply equations 3 to 5 to three β''/β-alumina peak couples for the different sintering conditions (Table S-1). For all approaches, the results for the β''-alumina content vary depending on the peak couple selected for analysis. As shown in the different rows of Table S-1, we obtain β''-alumina contents between 92% and 100% for the β''/β-alumina peaks couples 01<u>1</u>1/107, 02<u>1</u>0/107, and 01<u>1</u>1/206. The resulting average fraction over the peak couples is arbitrary as it depends on the weight given to a particular β-alumina reflection. In our case, the 107 reflection dominates the average. The β''-alumina fraction determined according to equation 3 depends on the reference pattern applied. This is because published data differ significantly in relative peak intensities (*e.g.* for Li-stabilized Na-β''-alumina, the 02<u>1</u>0 peak differs by a factor of ten between PDF 202728 and 200991). Furthermore, references structures like PDF 191173, which do not contain Li, are often used as β''_{ref} for Li-stabilized Na-β''-alumina ceramics [37][38]. Depending on the reference pattern, we determine β''-alumina fractions ranging from 92% to 99%, even for the same peak couple (*e.g.* 02<u>1</u>0/107, row 1 in Table S-1). Nevertheless, due to the small intensity of the peaks at 30.3 and 33.6° 2θ obtained for our samples, the average over the peak couples obtained for the β''-alumina fraction according to the different approaches vary only by 5%. More importantly, all approaches result in a constant and high β''-alumina fraction > 95% for all sintering conditions.

Table S1 *β''-alumina content calculated from equations 3-5 for different characteristic reflections couples and references patterns. A difference of 8% is obtained according to the chosen PDF references and characteristic reflections.*

Sintering conditions		Reflections		f(β'') (%)				
T_{max} (°C)	Dwell time (min)	β''-alumina	β-alumina	Equ. 3 β''_{ref}: PDF 191173 β_{ref}: PDF 250775	Equ. 3 β''_{ref}: PDF 202728 β_{ref}: PDF 84604	Equ. 3 β''_{ref}: PDF 200991 β_{ref}: PDF 84604	Equ. 4	Equ. 5
1550	5	01$\underline{11}$	107	94.9	92.0	98.6	93.2	92.7
		02$\underline{10}$	107	94.5	92.6	99.2	96.2	96.0
		01$\underline{11}$	206	100.0	100.0	100.0	100.0	100.0
			Average	**96.5**	**94.9**	**99.3**	**96.5**	**96.2**
1600	5	01$\underline{11}$	107	95.8	93.3	98.9	94.3	94.0
		02$\underline{10}$	107	95.2	93.5	99.3	96.6	96.5
		01$\underline{11}$	206	100.0	100.0	100.0	100.0	100.0
			Average	**97.0**	**95.6**	**99.4**	**97.0**	**96.8**
1660	5	01$\underline{11}$	107	97.4	95.9	99.3	96.5	96.4
		02$\underline{10}$	107	97.2	96.2	99.6	98.1	98.0
		01$\underline{11}$	206	100.0	100.0	100.0	100.0	100.0
			Average	**98.2**	**97.4**	**99.6**	**98.2**	**97.2**
1550	30	01$\underline{11}$	107	95.9	93.5	98.9	94.5	94.1
		02$\underline{10}$	107	95.2	93.4	99.3	96.6	96.5
		01$\underline{11}$	206	100.0	100.0	100.0	100.0	100.0
			Average	**97.0**	**95.6**	**99.4**	**97.0**	**96.9**
1600	30	01$\underline{11}$	107	97.8	96.5	99.4	97.0	97.0
		02$\underline{10}$	107	97.5	96.6	99.7	98.3	98.3
		01$\underline{11}$	206	100.0	100.0	100.0	100.0	100.0
			Average	**98.5**	**97.7**	**99.7**	**98.4**	**98.4**
1660	30	01$\underline{11}$	107	97.1	95.3	99.4	96.0	95.8
		02$\underline{10}$	107	96.5	95.2	99.7	97.6	97.5
		01$\underline{11}$	206	100.0	100.0	100.0	100.0	100.0
			Average	**97.9**	**96.8**	**99.7**	**97.9**	**97.8**
1400	240	01$\underline{11}$	107	96.5	94.5	99.1	95.3	95.1
		02$\underline{10}$	107	95.3	93.7	99.3	96.7	96.6
		01$\underline{11}$	206	100.0	100.0	100.0	100.0	100.0
			Average	**97.3**	**96.0**	**99.5**	**97.3**	**97.2**
1500	240	01$\underline{11}$	107	99.0	98.4	99.7	98.6	98.6
		02$\underline{10}$	107	98.8	98.4	99.8	99.2	99.2
		01$\underline{11}$	206	100.0	100.0	100.0	100.0	100.0
			Average	**99.3**	**98.9**	**99.9**	**99.3**	**99.3**
1550	240	01$\underline{11}$	107	98.4	97.4	99.6	97.8	97.7
		02$\underline{10}$	107	98.6	98.0	99.8	99.0	99.0
		01$\underline{11}$	206	100.0	100.0	100.0	100.0	100.0
			Average	**99.0**	**98.5**	**99.8**	**98.9**	**98.9**

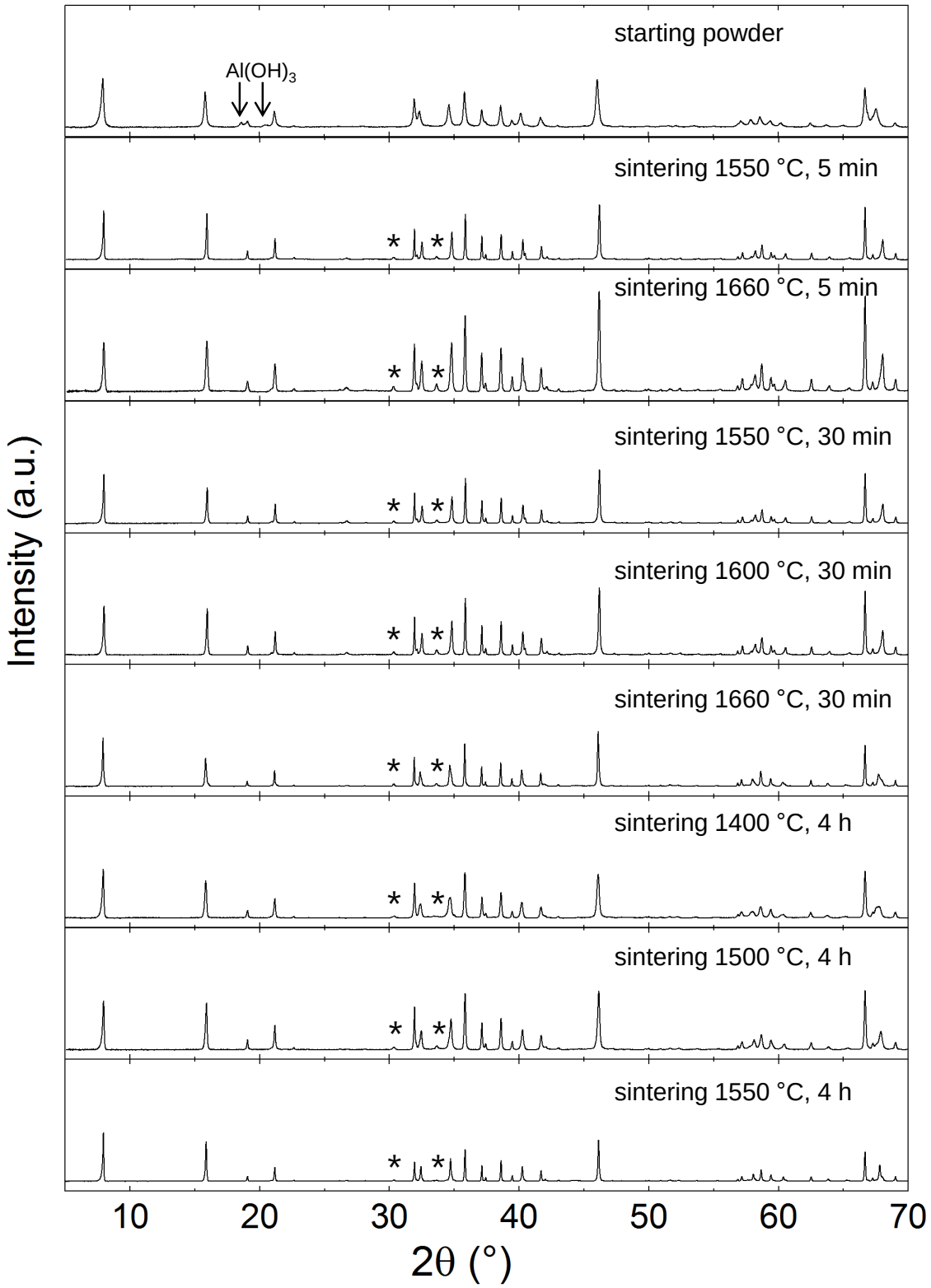

Figure S5 *Powder X-ray diffractograms of Na-β''-alumina powder and samples sintered at different conditions. Patterns normalized to the 003 reflection, additional reflections are marked.*

D. Estimation of Na_2O loss

We estimate the gas volume necessary to decrease the relative density for samples sintered for longer times at high temperatures by applying the ideal gas law *(PV = nRT)* assuming constant pressure. Consider the sample sintered at $T_1 = 1660$ °C for 30 min featuring 95% relative density (theoretical density is 3.27 g/cm^3). As an extreme case, we assume that this porosity is filled by pure Na_2O gas at this temperature. For a sample of 1 cm^3, this corresponds to a volume of gas $V_1 = 0.05$ cm^3 and a corresponding molar Na_2O content of $n_1 = n_0T_0V_1/T_1V_0 = 3 \cdot 10^{-7}$ mol, where n_0, T_0, V_0 are the standard gas conditions. Relative to the average Na_2O content in the sample of 14.3 ± 0.1 mol % (9.3 wt %), this corresponds to a decrease by 0.006 mol %, which is not detectable in our ICP-OES analyses. Similar results are also obtained when assuming lower temperatures of 1600 °C or 1500 °C for the closure of pores, which would correspond to a decrease by 0.006 mol % or 0.007 mol %.

E. Microstructure analysis

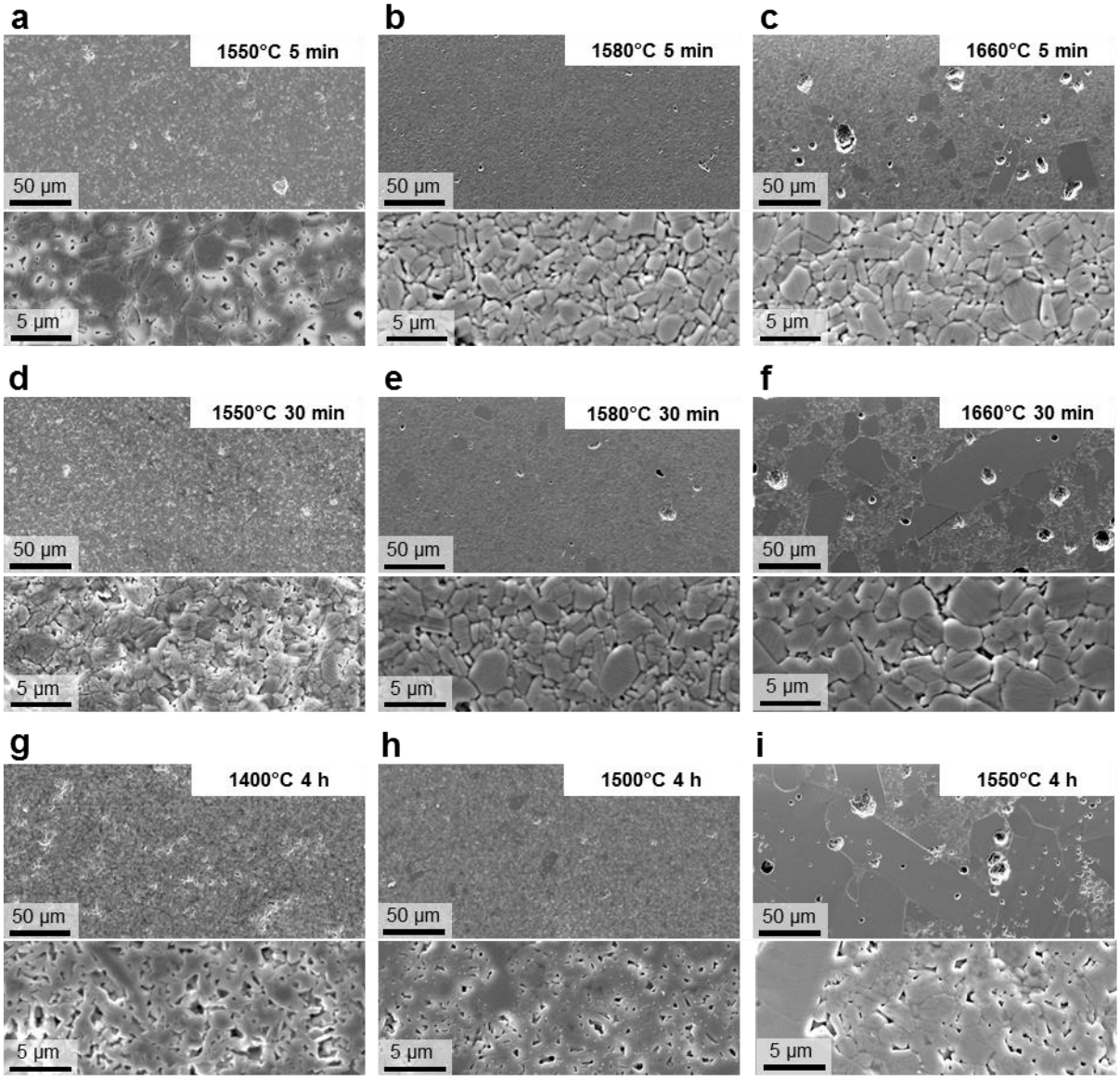

Figure S6 *Microstructures of samples sintered at different maximum temperatures and dwell time: (a) 1550 °C, 5 min (b) 1580 °C, 5 min (c) 1660 °C, 5 min (d) 1550 °C, 30 min (e) 1580 °C, 30 min (f) 1660 °C 30 min (g) 1400 °C, 4 h (h) 1500 °C, 4 h (i) 1550 °C, 4 h . At low temperature, the samples feature open porosity while at high temperatures or long dwell times, the samples feature abnormal grain growth.*

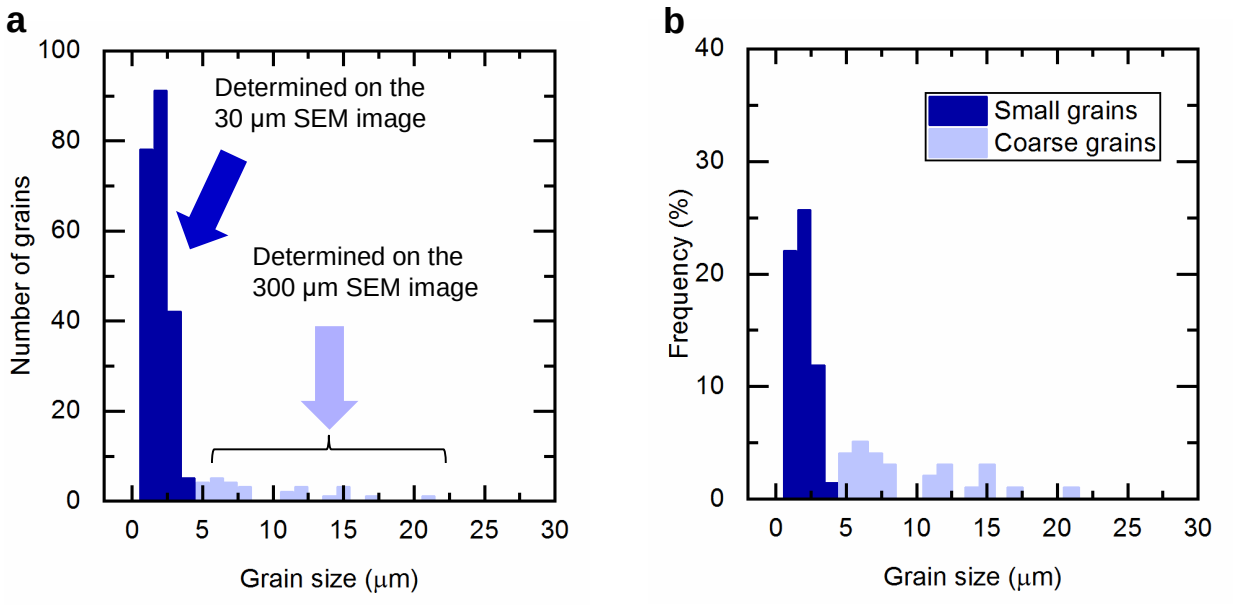

Figure S7 *Exemplary histograms of the bimodal grain size distribution of a sample featuring abnormal grain growth (sintered at 1660 °C for 30 min). (a) Number of grains and (b) frequency as a function of the grain size. In both cases, the bins are 1 μm large.*

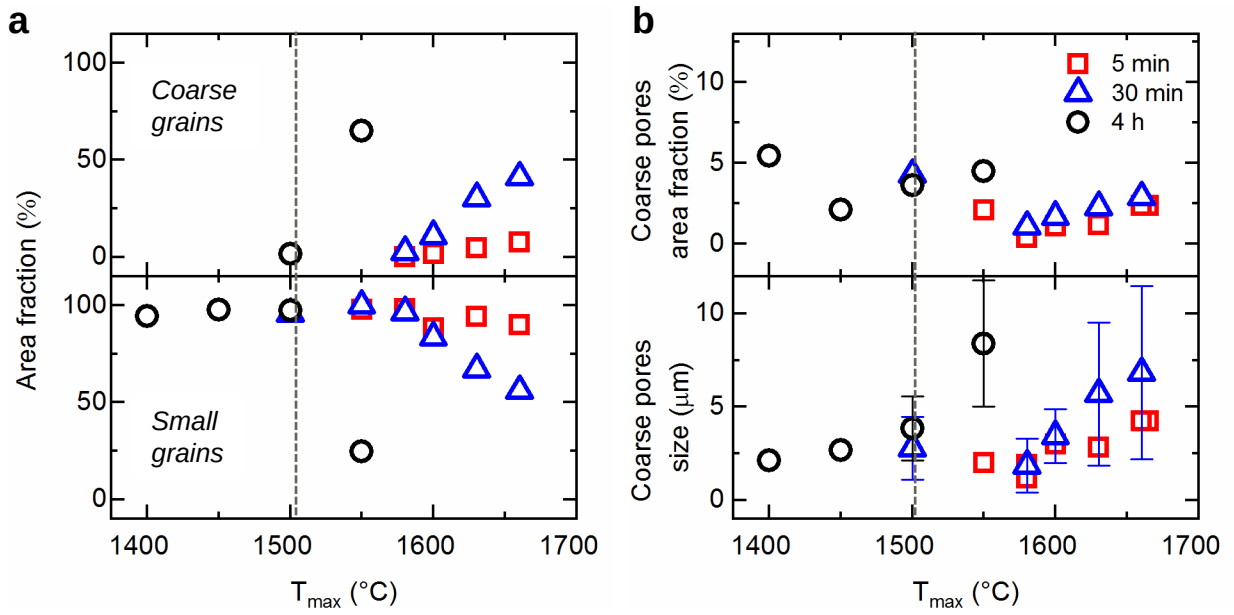

Figure S8 *(a) Area fraction of small and coarse grains and (b) coarse pores area fraction and size as a function of the sintering temperature (T_{max}) and for different dwell times. The dashed line indicates the onset of the liquid phase formation (≈ 1500 °C).*

References

[34] Eriksson, G.; Wu, P.; Pelton, A. D. Critical Evaluation of the Thermodynamic Properties and Phase Diamgrams of the MgO-Al_2O_3, MnO-Al_2O_3, FeO-Al_2O_3, Na_2O-Al_2O_3 and K_2O-Al_2O_3 Systems, CALPHAD, **1993**, *17*, 189-2015.

[35] Pekarsky, A.; Nicholson, P.S. The Relative Stability of Spray-Frozen/Freeze-Dried β″-Al_2O_3 Powders, *Mater. Res. Bull.* **1980**, *15*, 1517–1524.

[36] Duncan, G. K.; West, A. R.; Formation of Beta Alumina in the System Li_2O-Na_2O-Al_2O_3, *Solid State Ionics*. **1983**, *9–10*, 259–264.

[37] Zhu, C.; Hong, Y.; Huang, P. Synthesis and Characterization of NiO doped beta-Al_2O_3 Solid Electrolyte, *J. Alloys Compd.* **2016**, *688*, 746–751.

[38] Ahmadi Moghadam, H.; Hossein Paydar, M. The Effect of Nano CuO as Sintering Aid on Phase Formation, Microstructure and Properties of Li_2O-stabilized β″-Alumina Ceramics, *J. Ceram. Sci. Technol*. **2016**, *7*, 441–446.

[39] Chen, G.; Lu, J.; Zhou, X.; Chen, L.; Jiang, X. Solid-State Synthesis of High Performance Na-β″-Al_2O_3 Solid Electrolyte Doped with MgO, *Ceram. Int.* **2016**, *42*, 16055–16062.